Theoretical study of the metamagnetism in $ThCo_5$

Lars Nordström and Börje Johansson
Condensed Matter Theory Group, Department of Physics, University of Uppsala, Box 530, S-752 21 Uppsala, Sweden

Olle Eriksson
Center for Material Science, Los Alamos National Laboratory, Los Alamos, New Mexico 87544

M. S. S. Brooks
Commission of the European Communities, Institute for Transuranium Elements, Postfach 2340, D-7500 Karlsruhe, Federal Republic of Germany

(Received 15 May 1990)

A theoretical study of the magnetic properties of the intermetallic compound $ThCo_5$ has been performed by means of the fixed-spin-moment method. Metamagnetism is found in accordance with experimental observations, although only for slightly smaller volumes than the experimental equilibrium volume. It is found that for the lower magnetic state there are two distinctly different local cobalt magnetic moments, whereas for the higher magnetic state the two cobalt moments are nearly of the same size. These findings are discussed in terms of the calculated electronic structure. Appreciable orbital magnetic moments on the cobalt atoms are obtained when spin-orbit coupling is included in the calculations. The volume dependence of the theoretically calculated magnetic properties and its influence on the metamagnetic transition are discussed.

I. INTRODUCTION

The intermetallic compound $ThCo_5$ crystallizes in the hexagonal $CaCu_5$ structure. Although it is ferromagnetic at room temperature its cobalt magnetic moment is lower than those of the RCo_5 compounds (where R is a trivalent rare-earth element) with the same structure.[1] However, experiments have shown that $ThCo_5$ exhibits a transition from this low-moment state (LMS) to a high-moment state (HMS) with an applied magnetic field.[2,3] This is of considerable interest since it is one of the best examples of metamagnetism. Another, related, example of this phenomenon takes place in the cubic Laves compound YCo_2.[4] This compound has properties of an enhanced Pauli paramagnet, but its magnetic susceptibility shows an anomalous temperature dependence with a maximum at a finite temperature. It is commonly believed that this behavior is related to a metamagnetic instability, although the necessary field strength to accomplish the transition is too large to be achieved in the laboratory.[5,6] Measurements of the temperature dependence of the imposed susceptibility in $ThCo_5$ show the same shape as for YCo_2 with a maximum at finite temperature.

The general concept of itinerant metamagnetism was first proposed by Wohlfarth and Rhodes.[7] Since then Shimizu has extended the ideas and investigated more thoroughly the conditions for the occurrence of metamagnetic transitions.[8] In his work Shimizu discusses two special cases of metamagnetic transitions. The first case is when the transition goes from a paramagnetic to a ferromagnetic state when a magnetic field is applied, and the second case is when it goes from a ferromagnetic state to another ferromagnetic state with a higher magnetic moment. Accordingly, the metamagnetism of YCo_2 could be viewed as an example of the former case and that of $ThCo_5$ as an example of the latter form of transition. However, following the result of spin-polarized neutron-diffraction experiments on $ThCo_5$, which have shown that in the LMS the two cobalt sites have different local magnetic moments, whereas in the HMS the two moments are of the same size, there are arguments that the transition is occurring on only one of the two types of cobalt sites.[2,3] The cobalt atoms that exhibit this transition should then be paramagnetic before the transition, with only a small moment induced by the interatomic exchange field from the ferromagnetic cobalt atoms situated at the other type of sites. The metamagnetic transition should then correspond to that the paramagnetic cobalt atoms become ferromagnetic. The transition in $ThCo_5$ would accordingly be of the first type and related to the transition in YCo_2.

With the introduction of the so-called fixed-spin-moment (FSM) methods[5,9] *ab initio* electronic structure calculations have become a powerful tool to study itinerant metamagnetism. From the FSM calculations the total energy E emerges directly as a function of the magnetization M, if only spin contributions to the magnetism are taken into account. This is very convenient for discussions of metamagnetism and related phenomena. For instance, FSM was used to investigate theoretically the cubic Laves compound YCo_2,[5] where a metamagnetic state was found for a volume slightly smaller than the experimental one. FSM has also been extensively applied to explore phase transitions in the $3d$ transition elements.[10]

By calculating the total energy as a function of both magnetization and volume for different structures, it became possible to investigate the zero-temperature equation of states. This investigation showed that phase diagrams in terms of magnetization and volume are more complex than previously believed and several new phases were found.

In the present paper FSM calculations for $ThCo_5$ are reported. A review of the FSM method is given in Sec. II, while Sec. III contains computational details. The theoretical findings are presented in Sec. IV together with a discussion of the results and comparison with experimental data. Finally a summary is given in Sec. V.

II. THE FIXED-SPIN-MOMENT METHOD

The FSM method has been described before,[5] but it will be reviewed here to clarify the discussions of the results from the calculations. In an ordinary spin-polarized calculation based on the density functional theory[11] the ground state is obtained by minimizing the energy functional, E, with respect to the charge and magnetization densities, $\rho(\mathbf{r})$ and $\mu(\mathbf{r})$, under the constraint of a fixed number of particles, N. With the variational principle this corresponds to minimizing the functional

$$F[\rho(\mathbf{r}),\mu(\mathbf{r})]=E[\rho(\mathbf{r}),\mu(\mathbf{r})]-\mu\left[\int\rho(\mathbf{r})d\mathbf{r}-N\right], \tag{1}$$

where μ is a Lagrange multiplier, the chemical potential [not to be confused with the magnetization density $\mu(\mathbf{r})$]. The minimization gives

$$\frac{\delta E}{\delta\rho(\mathbf{r})}=\mu\ , \tag{2a}$$

$$\frac{\delta E}{\delta\mu(\mathbf{r})}=0\ . \tag{2b}$$

With a local approximation[12,13] to the exchange-correlation part of the energy functional these equations lead to effective one-electron equations which are solved by a self-consistent procedure.

When an external magnetic field, H, is taken into account, the variational principle gives the same equations although the effective one-electron potential has to be modified. By varying the strength of the field, the field dependence of the total energy and of the magnetization can be calculated straightforwardly. However, as the magnetization as a function of the applied field, $M(H)$, may be a multivalued function, there will be problems with the convergence in regions of H where more than one solution exist, i.e., for instance in the regions where metamagnetic transitions occur.

In the FSM method another approach to the problem is used. By adding a constraint[14] of a fixed spin moment, m_S, to Eq. (1) the problem will be to minimize the functional

$$F[\rho(\mathbf{r}),\mu(\mathbf{r})]=E[\rho(\mathbf{r}),\mu(\mathbf{r})]-\mu\left[\int\rho(\mathbf{r})d\mathbf{r}-N\right]-h\left[\int\mu(\mathbf{r})d\mathbf{r}-m_s\right]\ . \tag{3}$$

Here h is the Lagrange multiplier which applies the constraint of a fixed spin moment m_S. In the approximation that orbital contributions to the magnetization are neglected, which is usually appropriate for the $3d$ elements, the spin moment is directly related to the magnetization, $m_S=M/\mu_B$.

Instead of minimizing with respect to $\rho(\mathbf{r})$ and $\mu(\mathbf{r})$, it is more illustrative to change to the spin up, $\rho^+(\mathbf{r})$, and spin down, $\rho^-(\mathbf{r})$, densities

$$\rho^+(\mathbf{r})=\tfrac{1}{2}[\rho(\mathbf{r})+\mu(\mathbf{r})]\ , \tag{4a}$$

$$\rho^-(\mathbf{r})=\tfrac{1}{2}[\rho(\mathbf{r})-\mu(\mathbf{r})]\ . \tag{4b}$$

Then the variational principle yields

$$\frac{\delta E}{\delta\rho^+(\mathbf{r})}=\mu+h\ , \tag{5a}$$

$$\frac{\delta E}{\delta\rho^-(\mathbf{r})}=\mu-h\ . \tag{5b}$$

From a comparison with Eq. (2a) the right-hand sides of Eqs. (5a) and (5b), $\mu\pm h$, may be identified as chemical potentials for the two different spins. In general, however, $\mu\pm h$ will appear as constants added to the one particle potentials. The identification of $\mu\pm h$ as chemical potentials is only justified when the two spins are decoupled in the Hamiltonian matrix. This is not always the case, such as for example when spin-orbit coupling is included or when noncollinear magnetism[15] is considered because then the Hamiltonian matrices are not block diagonal in the spin.

Thus, the condition of having a fixed (spin) magnetic moment corresponds to using two different chemical potentials, i.e., two Fermi energies for a metal at zero temperature. This can also be seen from Eq. (3) which can be rewritten as

$$F[\rho(\mathbf{r}),\mu(\mathbf{r})]=E[\rho(\mathbf{r}),\mu(\mathbf{r})]-(\mu+h)\left[\int\rho^+(\mathbf{r})d\mathbf{r}-N^+\right]-(\mu-h)\left[\int\rho^-(\mathbf{r})d\mathbf{r}-N^-\right], \tag{6}$$

where N^+ and N^- are the numbers of particles of majority and minority spin, respectively. Therefore, the FSM method corresponds to fixing the number of particles of the two spins separately. The associated Fermi energies are then found from the relations

$$N^\sigma=\int_{-\infty}^{\varepsilon_F^\sigma}D^\sigma(\varepsilon)d\varepsilon\ , \tag{7}$$

where $D^\sigma(\varepsilon)$ and ε_F^σ are the density of states and the Fermi energy for spin σ, respectively.

Equations (5a) and (5b) lead to the same one-electron equations as for the ordinary case without an external magnetic field. There is, however, implicitly a field incorporated in the FSM method, as can be seen by

$$H=\left[\frac{\partial E}{\partial M}\right]_V=\left[\frac{\partial E}{\partial N^+}\frac{\partial N^+}{\partial M}+\frac{\partial E}{\partial N^-}\frac{\partial N^-}{\partial M}\right]_V=\frac{1}{2\mu_B}(\varepsilon_F^+-\varepsilon_F^-)=\frac{1}{\mu_B}h\ , \tag{8}$$

where E is the total energy obtained from the minimiza-

tion of Eqs. (3) or (6).

That there are two separate Fermi energies for the two spins in the FSM method does not mean that there is any close relationship to the conventional Stoner theory with rigid bands, where two separate Fermi energies also appear. There the different ε_F^σ are introduced not just for taking care of an applied field but in addition the often dominating intra-atomic exchange splitting, which in the FSM method is treated with the full strength of density functional theory in the local spin density approximation (LSDA).

III. DETAILS OF CALCULATION

In the calculations reported here the one-electron equations are solved with the linear muffin-tin orbital (LMTO) method in the atomic-sphere approximation (ASA) including the combined correction terms to ASA.[16] The LSDA exchange-correlation potential is parametrized according to von Barth and Hedin.[13] The irreducible part of the hexagonal Brillouin zone was sampled at 112 k points. A basis set of functions with angular momenta up to $l=3$ on all sites was adopted. This together with the fact that there are six atoms per unit cell give a dimension of 96 for the matrices to be diagonalized. As for the radii of the spheres for the different atoms, they were constructed in such a way that the ratio is kept equal to the ratio of the sphere radii of the elemental metals, i.e., $S_{Co}/S_{Th}=0.70$.

IV. RESULTS AND DISCUSSIONS

A. Total energy calculations

Due to the size of the present problem, no attempts have been made to calculate a general $E(M,V)$ relation as was done by Moruzzi *et al.*[10] for the 3d elements. Not only are the matrices ten times larger than for the 3d elemental metals, but due to the hexagonal structure of $ThCo_5$, the total energy has to be calculated in a three-dimensional parameter space, i.e., the lattice constants, a and c, together with the spin moment, m_S. Instead a simpler approach has been adopted. Thus $E=E(M)$ relations for three different volumes have been calculated, where only the c lattice parameter is varied. This constraint is a reasonable simplification since the a axis is considerably more rigid than the c axis for hexagonal ACo_5 intermetallic systems. The three volumes, together with the corresponding lattice parameters, are given in Table I. The largest volume (case c in Table I) is taken to be equal to the experimental value.[17] In Fig. 1 the FSM calculated $E(M)$ curves are shown. For the experimental volume (case c) there is only one minimum at $6.0\mu_B$ per unit cell. However, it can easily be recognized that there is a tendency to another minimum already at a magnetic moment of about $3.0\mu_B$/unit cell. For the smaller volumes (case a and case b) there exist two minima and for the smallest volume (case a) the minimum corresponding to the lowest moment, i.e., the LMS, actually also has the lowest total energy.

To obtain a better description of the metamagnetism, the variation of the difference between the Fermi energies

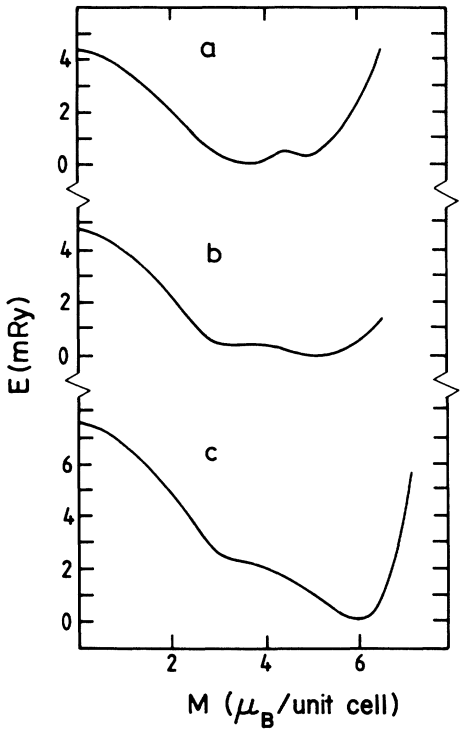

FIG. 1. The total energy, E, as a function of the magnetization, M, for volumes corresponding to the cases a, b, and c in Table I.

of the two spins, $\Delta\varepsilon_F=\varepsilon_F^- - \varepsilon_F^+$, with the magnetization, is shown in Fig. 2 for the three volumes. The difference in Fermi energies is related to the derivative of $E(M)$ as can be seen from Eq. (8).

$$\Delta\varepsilon_F(M)=-2h=-2\mu_B\left[\frac{\partial E}{\partial M}\right]_V . \tag{9}$$

Stable states without an external field exist only when $\Delta\varepsilon_F=0$ and its derivative, $\partial\Delta\varepsilon_F/\partial M$, is negative. These solutions then correspond to what can be calculated with an ordinary spin-polarized calculation, although there would be problems when several stable states exist (as for the volumes corresponding to cases a and b). At the experimental volume (case c) $\Delta\varepsilon_F$ has two nodes, i.e., besides the trivial solution $M=0$ there is also a solution at $M=6.0\mu_B$/unit cell. In addition to the two zero points for $\Delta\varepsilon_F(M)$, there is a minimum at $M=3.5\mu_B$/unit cell which corresponds to the tendency towards a minimum in the $E(M)$ curve mentioned above (cf. Fig. 1). This minimum in $\Delta\varepsilon_F(M)$ move down to just below zero for the volume corresponding to case b, which shows the ex-

TABLE I. The three volumes used in the calculations and the corresponding hexagonal lattice parameters.

	V (Å^3)	a (Å)	c (Å)
a	83.80	5.00	3.87
b	85.00	5.00	3.93
c	86.32	5.00	3.99

istence of a locally stable LMS for this volume. For the smallest volume (case *a*) the minimum remain below zero, but now the maximum beyond the minimum just reaches above zero. This indicates that for smaller volumes than that of case *a* there will only exist one stable state, namely the low magnetic state (LMS). This means that the metamagnetism of $ThCo_5$ will disappear with pressure. In fact, the calculations indicate that it is only for a relatively narrow range of volumes for which $ThCo_5$ is metamagnetic.

A comparison with experiments shows that the theoretical magnetic moments are all too small. The experimental LMS has a magnetic moment of $4.9\mu_B$/unit cell (Ref. 3) to be compared with the presently calculated values $3.2-3.5\mu_B$/unit cell, dependent on the volume. In the HMS a magnetic moment of $7.3\mu_B$/ unit cell (Ref. 3) have been measured which is larger than the calculated values, $5.0-6.0\mu_B$/unit cell. The discrepancy between theory and experiment can, at least partially, be attributed to the approximations used in the calculations. It is a well known experience that LDA calculations in ASA, or in a similar approximation, often give magnetic moments with an inaccuracy of about 5–10 %. In the present case, however, a major part of the discrepancy might be attributed to the neglect of orbital moments in the calculations. There are experimental data available which indicate unusually large orbital moments on the cobalt atoms in $ThCo_5$ (Ref. 18) and RCo_5 (Refs. 18 and 19) compounds. Calculations for RCo_5 systems including spin-orbit coupling have to some extent reproduced these orbital contributions to the magnetic moment.[20] For the two stable magnetic moments corresponding to the volume for case *b* spin-orbit coupling have been added to the calculations[16,21] and the induced orbital moments have been calculated in the same way as in Ref. 20 for the RCo_5 compounds. These calculated orbital moments are $0.72\mu_B$/unit cell and $0.62\mu_B$/unit cell for the LMS and the HMS, respectively, which reduces the discrepancy mentioned above between the theoretical and experimental total magnetic moments. It also agrees well with the experimental estimate[18] of $0.7\mu_B$/unit cell for the orbital moment.

Experimentally an applied field of about 80 kOe is needed to reach the HMS for $ThCo_5$.[2,3] Theoretically it is only for the smallest volume (case *a*) that LMS is the ground state and among the three investigated volumes it is therefore the only one for which a critical field exists. For that volume we have derived the relation between M and h which is shown in Fig. 3. This relation is obtained from Fig. 2(a) through an inversion of the relation $\Delta\varepsilon_F=\Delta\varepsilon_F(M)$. By means of a Maxwell construction, a critical value for the metamagnetic transition from the LMS to the HMS is found to be $h_C=0.1$ mRy, which corresponds to a magnetic field of 200 kOe. This value seems to be quite satisfactory when compared with the experiment. However, connected to a transition from LMS to HMS there is also an expansion in volume due to the loss in bonding associated with the increased magnetization. Therefore, in order to get a realistic estimate of

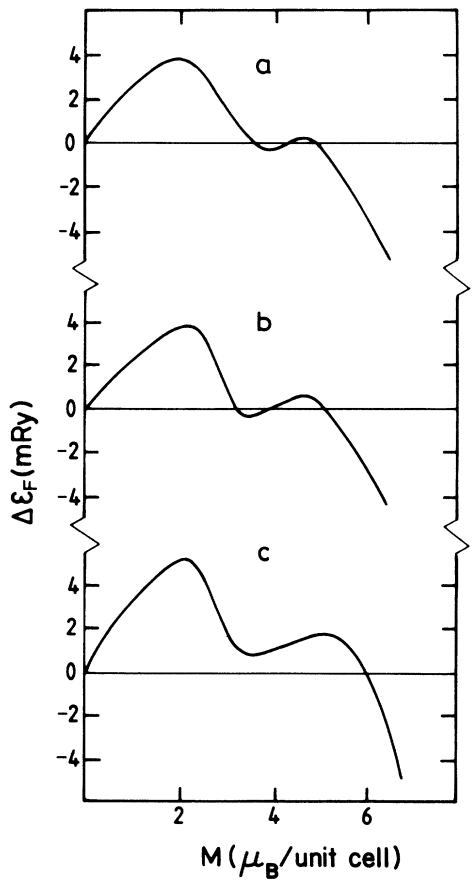

FIG. 2. The difference in Fermi energies, $\Delta\varepsilon_F=\varepsilon_F^- - \varepsilon_F^+$, as a function of magnetization, M, for the three volumes given in Table I.

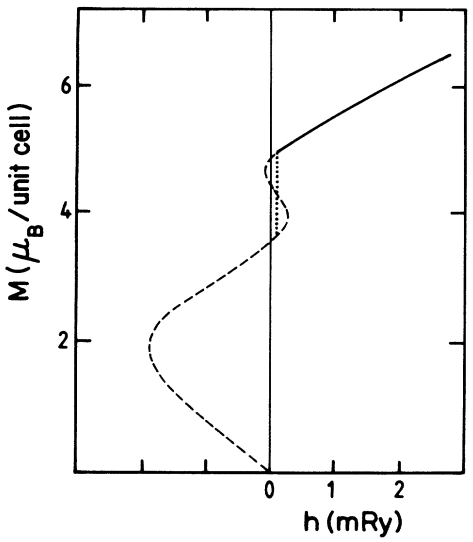

FIG. 3. The variation of the magnetization, M, with h. For positive values h is related to an applied field; $H=h/\mu_B$. The values of h which correspond to thermodynamically stable states are shown with full drawn line. The discontinuity corresponding to the metamagnetic transition is marked with a dotted line.

the critical field this change in volume should be incorporated in the theory. If the absolute values of the calculated total energies for the three volumes in Fig. 1 are considered, one obtains that the LMS at the volume for case *a* is lowest in energy and just below the HMS at the volume for case *c*. Assuming that these states also would be lowest in energy when the full $E(M,V)$ relation is known, then there would be a metamagnetic transition at a very small magnetic field (less than 100 kOe) with an accompanying volume expansion of 3%. This illustrates that with this relatively complex, hexagonal structure and the non-negligible magneto-volume coupling together with the inaccuracy inherent to the approximations used, a reliable, quantitative theoretical study of the metamagnetic transition as regards critical field and equilibrium volumes for $ThCo_5$ is very hard to achieve with the presently available calculational tools.

B. The electronic structure

In the $CaCu_5$ structure (Fig. 4) there are two inequivalent cobalt sites. The Co(1) site, with two atoms per unit cell, is situated in the basal plane and has the symmetry of the point group $\bar{6}m2$, while the Co(2) site, with three atoms per unit cell, is situated half way between two basal planes with the symmetry *mmm*. Due to the different local environments the site projected densities of states (DOS) of the two sites are somewhat different. This can perhaps most easily be seen for the paramagnetic ($M=0$) DOS. In Fig. 5 the total DOS for the volume of case *a* is shown. The dominating feature is the cobalt 3*d* bands, which range from about 4 eV below to about 1 eV above the Fermi level, ε_F. Thus the cobalt 3*d* bandwidth is about 5 eV. In Fig. 5 is also shown the difference of the projected DOS for the 3*d* states of the two different types of cobalt sites. There one can see that for a range from 1.7 to 0.7 eV below ε_F the Co(2) 3*d* states has a larger contribution to the DOS than the Co(1) 3*d* states, whereas from 0.7 eV below to 0.2 eV about ε_F the dominating part derives from the Co(1) 3*d* states. However, due to the very strong mixing (hybridization) between the states of the two different types of cobalt sites, there are

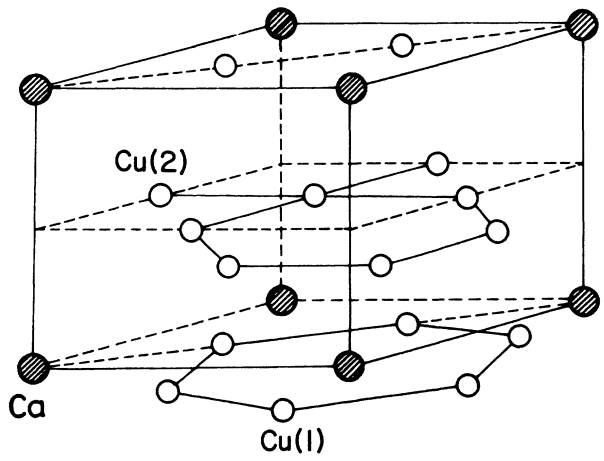

FIG. 4. The $CaCu_5$ crystal structure.

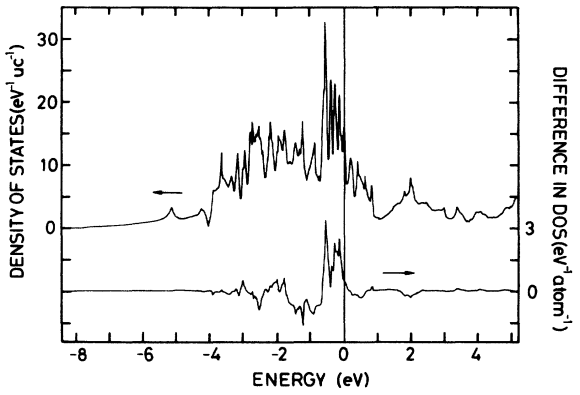

FIG. 5. The total density of states (left-hand scale) and the difference between the site projected 3*d* DOS of the two types of cobalt sites; DOS [Co(1)-3*d*]–DOS[Co(2)-3*d*] (right-hand scale). The Fermi energy is marked with a vertical line at zero energy.

contributions from both types to the total DOS throughout the whole range of the 3*d* bands. There is also a far from negligible hybridization between the cobalt 3*d* states and the 6*d* states of thorium. This hybridization introduces some Th 6*d* character into what we call the 3*d* bands but which constitutes the bonding part of the 6*d*-3*d* hybridization complex formed. Since the Th 6*d* occupation number is 2.2 in $ThCo_5$ this hybridization can be regarded as stronger than the corresponding one in, for instance, $LaCo_5$, where the La 5*d* occupation number is 1.6. This stronger intermixing of the Th 6*d* states into the bonding complex gives rise to a smaller magnetic moment in $ThCo_5$ than in $LaCo_5$. Another effect of the hybridization is the broadening of the bands involved. The difference in strength of the hybridization between $ThCo_5$ and $LaCo_5$ is reflected in the fact that the bandwidth of the 3*d* bands are about 0.5 eV larger in $ThCo_5$ than in $LaCo_5$. These broader bands, in turn, are also partially responsible for the weaker 3*d* magnetization in $ThCo_5$ than in the RCo_5.

The 3*d* DOS of Co(1) predominates at the Fermi level, 2.7 states /eV atom compared to 2.1 states /eV atom (case *a*) for Co(2). It is the states close to the Fermi energy that are responsible for whether the paramagnetic state is stable or not. This is summarized in the Stoner criterion for the instability of a paramagnetic state towards ferromagnetism,[22] $IN(\varepsilon_F)>1$, where I is the Stoner parameter[23] and N the DOS per spin. For $ThCo_5$ a Stoner product of, $IN(\varepsilon_F)=1.05$, is calculated which confirms that the paramagnetic state is unstable. (This number is calculated for a volume corresponding to case *a*, but very similar values were also found for the other volumes.) If one separates the contributions from the different sites, one can define local Stoner products.[20] The local Stoner products are calculated to be 1.26 and 0.98 for the Co(1) and Co(2) sites, respectively. This indicates that it is the Co(1) site that drives the compound into the ferromagnetic state, but the Co(2) site is also by itself on the verge to an instability.

In Fig. 6 the local cobalt moments are shown as a function of the total magnetic moment for the volume corresponding to case *b*. Their behavior at small M confirms the results for the local Stoner products. Corresponding curves for the other two volumes (cases *a* and *c*) have the same overall shape and have values within 10% of the curves shown. As can be seen from the figure for small total moments almost the entire moment lies on the Co(1) site. Since there is a strong hybridization between the 3*d* states of the two sublattices, the spin splittings of the Co(1) and Co(2) bands are connected, which is reflected in the fact that above a total moment of about $2\mu_B$/unit cell the increase in the total magnetic moment is shared more equally between the two types of cobalt sites. When the total moment reaches $6\mu_B$/unit cell the moments of the two different cobalt sites have become almost equal. The reason for this can be extracted from the DOS for the FSM calculation for $M=6\mu_B$/unit cell in Fig. 7. There one notices that the spin splitting has now become so large that the 3*d* bands of the majority spin are fully occupied for both types of sites. This specifies the HMS as a strong magnetic state, where the local moments of both types of cobalt sites are saturated. This is in accordance with the very steep upturn of the total energy for M above $6\mu_B$/unit cell in Fig. 1, where the magnetic moment already is saturated. Also shown in Fig. 6 are the individual magnetic moments where the orbital part is included for the theoretically stable states. (Notice that when an orbital contribution to the magnetic moment is included both the local magnetic moments, m_i, increase, although the values with orbital moment included lies below the spin-only curve for type-II sites in Fig. 6. This is due to the fact than an orbital part is now included in the total magnetization, M.) The orbital moment is larger on site I for both the LMS and the HMS. This is especially pronounced for the LMS where it is $0.28\mu_B$/atom for site I and only $0.05\mu_B$/atom for site II. This very large orbital moments on the Co(1) site in the LMS may be related to the experimental finding of a large anisotropy in the LMS.[3]

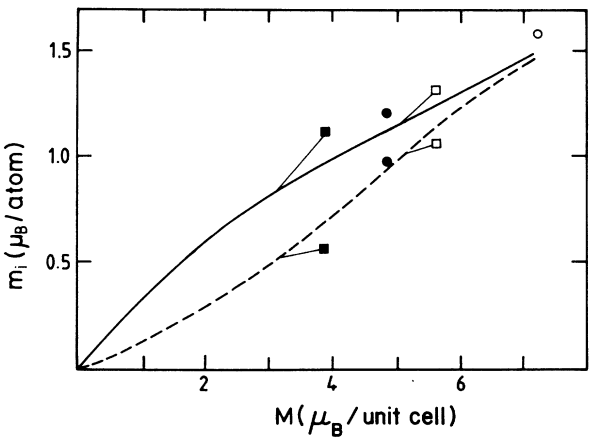

FIG. 6. The variations of the local spin magnetic moments, m_i, with the total magnetization, M, for the Co(1) type of site (full drawn line) and the Co(2) type of site (dashed line), for a volume corresponding to case *b* in Table I. Also shown are the results from calculations with spin-orbit coupling included for the two stable states; the so obtained LMS magnetic moments are shown with solid squares and the HMS magnetic moments are shown with open squares. Thin lines are used to connect these values with the corresponding values where only spin moments are considered. Included, for comparison, are also experimental data (Refs. 2 and 3) for both the LMS (solid circles) and the HMS (open circle).

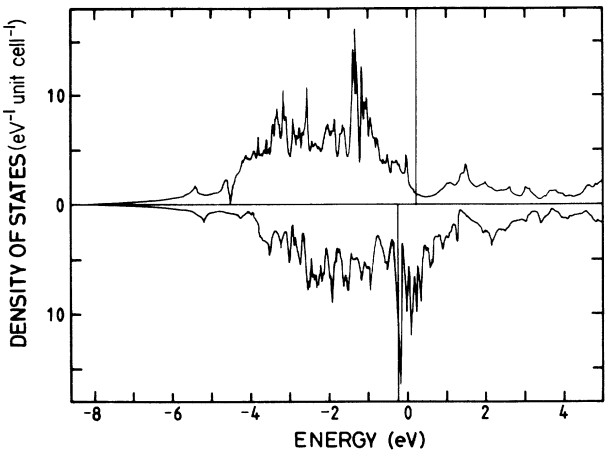

FIG. 7. The spin-polarized DOS from a calculation performed at a volume corresponding to case *a* in Table I. The DOS of the majority spin is above the zero line and the DOS of the minority spin is below. The two Fermi energies are marked with vertical lines. Zero energy is the average of the two Fermi energies.

For a comparison the experimental values[2,3] for the LMS and HMS are also shown in Fig. 6. As already mentioned the local magnetic moments of the two cobalt sites are different in the LMS but almost equal in the HMS. There is a clear correspondence between these values and the theoretical curve.

Figure 8 shows the DOS around the Fermi energy for the two stable states for the volume of case *b*. There one can see that for the minority spin states the Fermi levels are situated in valleys of the DOS, which is in accordance with the conditions for metamagnetism.[7,8] In the transition from the LMS to the HMS a peak in the DOS of the minority spin is pulled from below to above the Fermi energy. For the majority spin the Fermi levels are situated in almost flat regions of the corresponding DOS, with almost equal contributions from the two types of cobalt sites. Since the peak in the minority spin DOS, which passes the Fermi level in the metamagnetic transition, is of more Co(1) character than Co(2) character per atom, one would be inclined to believe that the magnitude of the local magnetic moment of Co(1) will increase more in the transition than that of Co(2). However, such an argument is implicitly based on an assumption of rigid bands. The fact that the DOS is not rigidly shifted in the transition can easily be verified by a direct comparison between the two panels in Fig. 8. Instead the charge and magnetization densities go through a relaxation, which causes changes in the DOS. This complex mechanism seems to

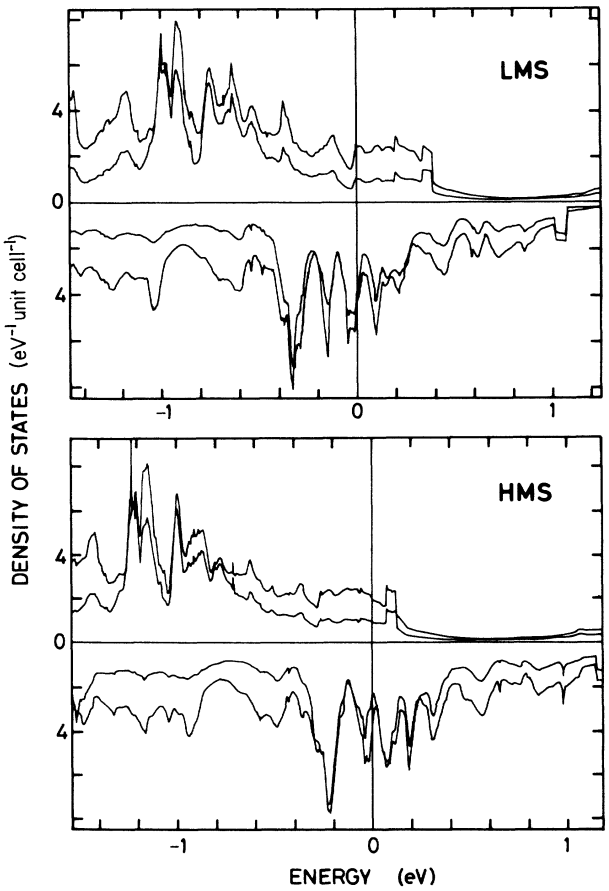

FIG. 8. Expanded view of the spin-polarized site projected 3*d* DOS for energies close to the Fermi energies for the two stable magnetic states, $3.2\mu_B$/unit cell (top panel) and $5.0\mu_B$/unit cell (bottom panel), calculated at the volume corresponding to case *b* in Table I. The majority (minority) spin states are those shown above (below) the zero line. Because there are more atoms of Co(2) type per unit cell than there are of Co(1) type, the DOS of Co(2) is the one that dominates most of the energy range shown.

prevent any attempts to explain the transition in any simple way. However, as the local Co(1) moment is closer to saturation than the Co(2) moment in the LMS and both are almost saturated in the HMS, it is obvious that the largest effect of the metamagnetic transition occurs on the Co(2) sites.

V. SUMMARY

When calculating the total energy as a function of the magnetic moment for $ThCo_5$ for volumes slightly smaller than the experimental one, two locally stable states with different magnetic moments were found in agreement with the experimental claim of metamagnetism in this compound. However, at the experimental volume the LMS was actually not found, only a minimum in $\Delta\varepsilon_F(M)$ at about $3.5\mu_B$/unit cell indicates the closeness to such a state. The HMS was calculated to be situated at $6.0\mu_B$/unit cell and can be assigned as strongly magnetic with saturated cobalt moments. Although we do not find two energy minima at the experimental volume the magnetic moments for the two magnetic states (of which the LMS is hypothetical) for this volume are closer to the experimental values[2,3] than those we calculate for smaller volumes. Especially if our calculated orbital contributions are added to these values a good agreement is found, $4.2\mu_B$/unit cell to be compared to the experimental value $4.9\mu_B$/unit cell for the LMS and $6.6\mu_B$/unit cell to be compared to the experimental value $7.3\mu_B$/unit cell for the HMS. Thus at the experimental volume the calculated magnetic moments seem to be in good correspondence with the experimental data.

An important aspect of a metamagnetic transition is the critical field needed to accomplish it. From the FSM calculation for the volume of case *b* the critical field is estimated to be about 200 kOe. However, as there is a magneto-volume effect involved in the transition, a more realistic estimation would require a complete knowledge of the $E(M,V)$ relation. From the minimal sampling of that relation which have been calculated in the present work a very small critical field is estimated for a transition that involves an expansion in volume of about 3%. In that estimation, however, the LMS has a 3% smaller volume than the experimental equilibrium volume. This is of an accuracy typical for calculations within the LSDA. This limited accuracy might be crucial when properties such as critical fields of metamagnetic transitions, which involves appreciable changes in volume, is calculated. Therefore further experimental investigations of the pressure dependence of the metamagnetic transition in $ThCo_5$ together with a detailed determination of the predicted lattice expansion involved in the transition could provide a good basis for a critical examination of the accuracy of the LSDA and its treatment of magneto-volume effects. Hitherto LSDA calculations of magneto-volume effects in magnetic transitions often have to be compared to experimental data from experiments performed at elevated temperature around the Curie temperature. These nonzero temperatures introduce physical phenomena, such as for instance spin fluctuations, which are not incorporated in the present theory. Thus it seems important that the metamagnetism in $ThCo_5$ will be studied experimentally at low temperature where the theoretical treatment involving ground-state properties is adequate. Very recently, the effects of pressure on the critical field of the metamagnetic transition in $ThCo_5$ has been reported.[24] It is found that there is a large increase in the critical field with an applied pressure. This indicates a strong volume dependence of the metamagnetic transition, which is consistent with our theoretical result.

To get a picture of the electronic structure underlying the metamagnetism of $ThCo_5$, densities of states for the two stable states at the volume corresponding to case *b* was shown in Fig. 8. There one could see that for the LMS the Fermi level was situated in a region with low density of states but with a large curvature, in correspondence with the necessary conditions for metamagnetism put forward by Wohlfarth and Rhodes.[7] The results from our present calculations support one of the conjectures given in connection with the interpretation of the

experimental results,[2,3] namely that the transition takes place mainly on one of the two crystallographically different cobalt sites. However, it is difficult to agree with the assignment[2,3] that the site II is basically paramagnetic in the LMS. The strong mixing between the 3*d* states of the two sites creates a strong coupling between the local magnetic moments. Although the contribution to the DOS around ε_F is larger from site I than from site II in the hypothetical paramagnetic state (see Fig. 5), and therefore the response to a small field is larger for site I than site II, the magnetic moments corresponding to the LMS both have an appreciable size. However, it is true that for the LMS the contribution to the DOS at the Fermi level is smaller for site II than for site I. Therefore the response to a magnetic field is weaker for that site, which might be the cause to the experimental observations that lead to the hypothesis that site II should be paramagnetic. Hence, the metamagnetic transition in $ThCo_5$ is found to be from one ferromagnetic state to another thus it belongs to the second case discussed by Shimizu.[8]

From the variation of the local cobalt moments with the fixed spin moment (cf. Fig. 6) one can instead attribute the finding of two unequal cobalt moments of the LMS to the fact that the magnetic moment of site I increases faster in magnitude for small magnetizations than the magnetic moment of site II does. This could in turn be attributed to the difference in the site projected DOS at the Fermi level (see lower panel in Fig. 5). On the other hand, the fact that the local cobalt moments are almost equal in HMS could be ascribed to the fact that in this case the cobalt moments are both saturated; i.e., the majority spin 3*d* bands for both sites are fully occupied. With increasing magnetization the saturation of the cobalt moments occurs first on site I which leads to that for larger magnetizations the increase of the magnetic moment has to take place mainly on site II. Therefore for magnetizations corresponding to the HMS both types of sites show saturated moments.

ACKNOWLEDGMENTS

Lars Nordström and Börje Johansson are thankful for the financial support from the Swedish Natural Science Research Council.

[1]W. A. J. J. Velge and K. H. J. Buschow, J. Appl. Phys. **39**, 1717 (1968).
[2]D. Givord, J. Laforest, and R. Lemaire, J. Appl. Phys. **50**, 7489 (1979).
[3]D. Givord, J. Laforest, R. Lemaire, and Q. Lu, J. Magn. Magn. Mater. **31–34**, 191 (1983).
[4]For a review, see for instance, W. Steiner, J. Magn. Magn. Mater. **14**, 47 (1979).
[5]K. Schwarz and P. Mohn, J. Phys. F **14**, L129 (1984).
[6]H. Yamada and M. Shimizu, J. Phys. F **15**, L175 (1985).
[7]E. P. Wohlfarth and P. Rhodes, Philos. Mag. **7**, 1817 (1962).
[8]M. Shimizu, J. Phys. (Paris) **43**, 155 (1982).
[9]A. R. Williams, V. L. Moruzzi, J. Kübler, and K. Schwarz, Bull. Am. Phys. Soc. **29**, 278 (1984).
[10]V. L. Moruzzi, P. M. Marcus, K. Schwarz, and P. Mohn, Phys. Rev. B **34**, 1784 (1986); P. M. Marcus, V. L. Moruzzi, and K. Schwarz, Mat. Res. Symp. Proc. **63**, 117 (1985); V. L. Moruzzi, Phys. Rev. Lett. **57**, 2211 (1986).
[11]P. Hohenberg and W. Kohn, Phys. Rev. **136**, B864 (1964).
[12]W. Kohn and L. J. Sham, Phys. Rev. **140**, A1133 (1965).
[13]U. von Barth and L. Hedin, J. Phys. C **5**, 1629 (1972).
[14]For a discussion of constraints in density-functional theory, see, P. H. Dederichs, S. Blügel, R. Zeller, and H. Akai, Phys. Rev. Lett. **53**, 2512 (1984).
[15]J. Kübler, K. -H. Höck, J. Sticht, and A. R. Williams, J. Phys. F **18**, 469 (1988).
[16]O. K. Andersen, Phys. Rev. B **12**, 3060 (1975).
[17]P. Villars and L. D. Calvert, *Pearson's Handbook of Crystallographic Data for Intermetallic Phases* (American Society for Metals, Metals Park, OH, 1986).
[18]A. Heidemann, D. Richter, and K. H. J. Buschow, Z. Phys. B **22**, 367 (1975).
[19]J. Schweizer and F. Tasset, J. Phys. F **10**, 2799 (1980).
[20]L. Nordström, O. Eriksson, M. S. S. Brooks, and B. Johansson, Phys. Rev. B **41**, 9111 (1990).
[21]M. S. S. Brooks and P. J. Kelly, Phys. Rev. Lett. **51**, 1708 (1983).
[22]E. C. Stoner, Proc. R. Soc. London, Ser. A **154**, 656 (1936).
[23]S. H. Vosko and J. P. Perdew, Can. J. Phys. **53**, 1385 (1975); O. Gunnarson, J. Phys. F **6**, 587 (1976); J. F. Janak, Phys. Rev. B **16**, 255 (1977).
[24]R. Ballou, M. Shimizu, and J. Voiron, J. Magn. Magn. Mater. **84**, 23 (1990).